Journal of Luminescence 168 (2015) 192–198

Contents lists available at ScienceDirect

Journal of Luminescence

journal homepage: www.elsevier.com/locate/jlumin

Photoinduced electron and energy transfer within a pyrene-perylenediimide dyad embedded in polymer matrixes

Wenmiao Chen, Zhen Dai, Haiquan Liu, Heyuan Liu, Yan Shi, Xiyou Li *

Department of Chemistry, Shandong University, Jinan 250100, China

ARTICLE INFO

Article history:
Received 9 May 2015
Received in revised form
11 July 2015
Accepted 27 July 2015
Available online 11 August 2015

Keywords:
Electron transfer
Energy transfer
Pyrene
Perylenediimide
Polymer matrix

ABSTRACT

To investigate the effects of polymer matrixes on the competition between energy and electron transfer, a covalently linked pyrene-perylenediimide dyad (**PDI-PY**) has been prepared. Competition between the energy and electron transfer from PY to PDI within **PDI-PY** is revealed by steady state absorption and fluorescence spectra, as well as time resolved fluorescence spectra. Polar solvents accelerate the electron transfer while non-polar solvents favor the energy transfer. When **PDI-PY** is embedded in a non-polar polymer matrix, the energy transfer becomes the only photoinduced process between PY and PDI, whereas the electron transfer is almost completely hindered. In a polar polymer matrix, the energy transfer is still a dominating process, but with a remarkably decreased efficiency. The electron transfer in a polar polymer matrix is much slower and less efficient with respect to that in solutions, but faster and more efficient than that in non-polar polymer matrixes. This result suggests that polymer matrixes are ideal environment for constructing light harvesting systems, which in some case can reduce the disturbance from electron transfer.

1. Introduction

Photoinduced electron and energy transfer are the fundamental processes in natural photosynthesis [1–3] as well as in some other important photo-driven processes [4–6]. For example, electron transfer is an essential process for photoelectric conversion in solar cells [4,5] and photodegradation of pollutants [6]. Hence, exploring the mechanisms that govern the process of photoinduced energy and electron transfer between/among donors and acceptors became one of the most active fields of physical chemistry during the past several decades [7–11]. Besides the molecular structure, environment can also affect photoinduced electron and energy transfer remarkably. This environment sensitivity of photoinduced processes provides opportunities to control the photoinduced process by different outer stimulus. Based on this environment sensitivity, various fluorescence sensors or probes were developed [12–16].

Efficient intramolecular electron or energy transfer in both optoelectronic devices and natural photosynthesis normally occurs in the solid state [1,4]. Due to the difference on the microenviroment between solution and solid state, photoinduced electron and energy transfer processes are expected to change significantly when a molecule goes from solution to solid state [17]. The information about how the photoinduced electron and energy transfer change in solid state in comparison with that in solution is crucial for the design of efficient optoelectronic devices. However, the intramolecular photoinduced electron and energy transfer in solid environment, especially the competition between energy and electron transfer within a molecule in solid environment is scarcely reported in literatures [18].

In the present work, we compared the photoinduced electron and energy transfer between a covalently linked pyrene (PY) and perylenediimide (PDI) (**PDI-PY** in Fig. 1) in solutions with that in polymer matrixes. The reason we choose these two dye molecules as donor–acceptor pair is because both electron and energy transfer can happen efficiently between them [19–25]. The study on the photoinduced process of this kind of compound in solid films will give plenty information about the effects of a solid environment on photoinduced processes between a donor and an acceptor and help us to understand why the nature chose a solid state-like environment for photosynthesis.

2. Experimental

2.1. Reagents

Polystyrene (PS) and polymethylmethacrylate (PMMA) were purchased from commercial source and used as received without further purification. 1-(4′-hydroxyl-n-butyl) pyrene (**PY-OH**) was

* Corresponding author.
E-mail address: xiyouli@sdu.edu.cn (X. Li).

http://dx.doi.org/10.1016/j.jlumin.2015.07.046
0022-2313/

purchased from commercial source and purified by recrystallization from toluene before use. All other chemicals were of analytical grade.

2.2. Synthesis

1-hexyloxyl-3,4;9,10-tetracarboxylic diimide (**PDI-H**) was synthesized following the method of literature [26]. The molecular structure was characterized by ^{1}H NMR and ESI (Q-TOF) mass spectra. Pyrene-perylenediimide dyad (**PDI-PY**) was synthesized following the procedures for the synthesis of other similar compounds reported in our previous works [26,27], Scheme 1. The detailed synthetic procedures can be found in the Supplementary material. The molecular structure characterization results are summarized as below.

PDI-H

^{1}H NMR ($CDCl_3$): δ 9.57 (*d*, *J*=6.3 Hz, 1H), 8.56(m, 5H), 8.40 (s, 1H), 5.05 (m, 2H), 4.49 (*t*, *J*=4.9 Hz, 2H), 2.58 (m, 4H), 2.11 (*t*, *J*=5.5 Hz, 2H), 1.93 (*d*, *J*=8.6 Hz, 4H), 1.78 (*t*, *J*=9.5 Hz, 6H), 1.64 (*d*, *J*=5.9 Hz, 2H), 1.45 (m, 11H) 0.96 (*t*, *J*=5.3 Hz, 3H). ESI-MS (Q-TOF): Calcd. for $C_{42}H_{44}N_2O_5$: 656.33; Found: 656.30 (M^+).

PDI-PY

^{1}H NMR ($CDCl_3$): 9.24 (*d*, *J*=6.3 Hz, 1H), 8.52 (m, 2H), 8.29 (m, 2H), 8.21 (*d*, *J*=6.1 Hz, 1H), 7.95 (*d*, *J*=6.9 Hz, 1H), 7.87 (m, 3H), 7.75 (m, 5H), 7.56 (*d*, *J*=6.9 Hz, 1H), 5.06 (m, 2H), 4.36 (*d*, *J*=4.0 Hz, 2H), 3.39 (s, 2H), 2.62 (m, 4H), 2.21 (s, 4H), 1.97 (*d*, *J*=8.5 Hz, 4H), 1.85 (*d*, *J*=9.4 Hz, 4H), 1.79 (*d*, *J*=9.1 Hz, 2H). ESI-MS (Q-TOF): Calcd. for $C_{56}H_{48}N_2O_5$: 828.36; Found: 828.94 (M^+).

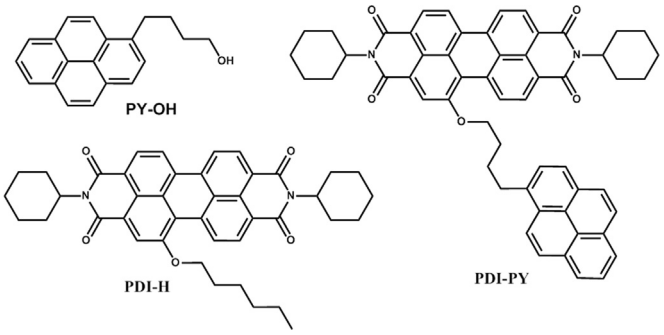

Fig. 1. Molecular structure of **PDI-PY** and model compounds.

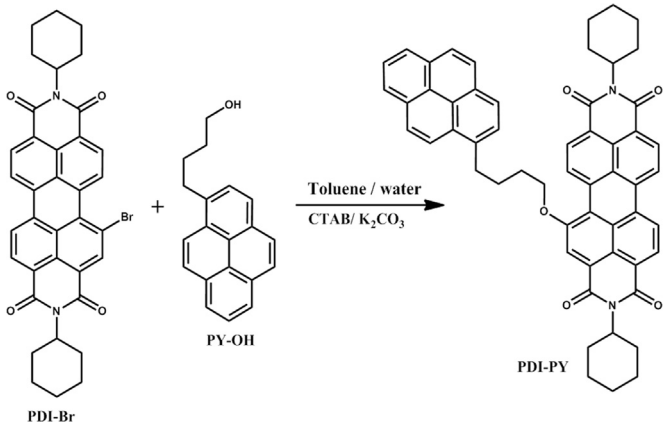

Scheme 1. Synthesis of **PDI-PY**.

2.3. Apparatus and methods

Electronic absorption spectra were recorded on a UV-2450 spectrophotometer (Shimadzu, Japan). The steady-state fluorescence measurements were carried out on a FLS920 fluorescence spectrometer (Edinburgh Instruments). The absolute fluorescence quantum yields were measured by an integrating sphere. The fluorescence lifetimes were measured with time correlated single photon counting (TCSPC) methods. ESI-MS were measured on Q-TOF LC/MS 6510 (Agilent). ^{1}H NMR spectra were recorded on a Bruker 300 MHz NMR spectrometer with the solvent peak as internal standard (in $CDCl_3$). The transparent thin solid films for the spectroscopic measurement are prepared by mixing a chloroform solution of samples with a chloroform solution of polymer and dropping the mixture to the cleaned surface of a glass substrate and evaporating the solvents at ambient conditions.

3. Results and discussions

3.1. Steady state absorption and fluorescence spectra in solutions

The absorption spectra of **PDI-PY** in toluene are shown in Fig. 2. The absorption spectra of this compound in other solvents are shown in Supplementary material (Fig. S3). There two groups of absorption bands in the absorption spectra of this compound in solution. The absorption bands in the long wavelength region (450–600 nm) can be ascribed to the absorption of perylenediimide (PDI) part of **PDI-PY**. The band with the absorption maximum appears at 545 nm can be assigned to the 0–0 vibronic band of the first excited state, while the band around 515 nm can be assigned to the 0–1 vibronic band [28–30]. The multiple absorption bands in the region of 250–360 nm can be assigned to the absorption of pyrene part of **PDI-PY** [31,32]. The absorption spectrum of **PDI-PY** is identical to the sum of the absorption spectra of model compound **PY-OH** and **PDI-H** at the same concentration. This indicates no ground state interaction between PDI part and PY part within **PDI-PY**. The absorption spectra of **PDI-PY** in different solvents of different polarities are identical, which means the polarity of solvent does not affect the absorption spectrum significantly, and suggests that the environmental change can not induce significant ground state interaction between the PDI and PY within **PDI-PY**.

The fluorescence spectra of **PDI-PY** in different solvents with excitations at 330 and 500 nm are shown in Fig. 3A and B, respectively. When **PDI-PY** is selectively excited at 500 nm, where

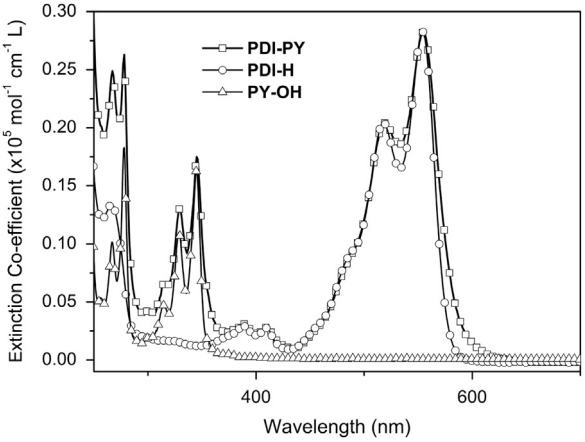

Fig. 2. Comparison of the absorption spectra of **PDI-PY** with that of model **PY-OH** and **PDI-H** in toluene.

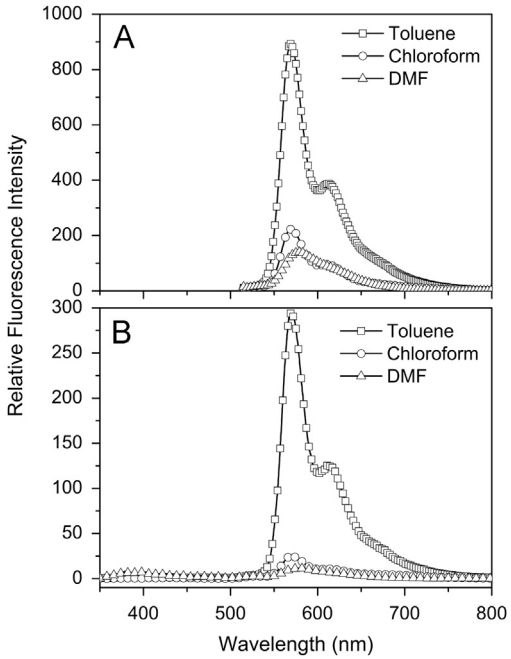

Fig. 3. The fluorescence spectra of **PDI-PY** in different solvents (10^{-6} M). (A) Excited at 500 nm. (B) excited at 330 nm. The spectrum with solid square in (B) is the fluorescence of model compound **PY-OH**.

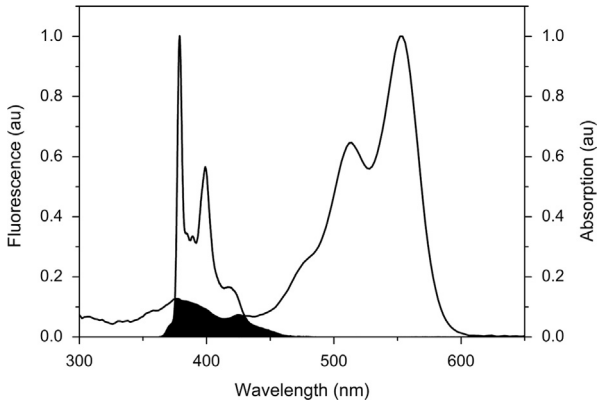

Fig. 4. Overlap between the absorption spectrum of **PHI-H** and the fluorescence spectrum of **PY-OH**.

only the PDI part absorbs light, **PDI-PY** in toluene shows typical fluorescence of PDI with the maximum emission band at about 560 nm as shown in Fig. 3A [33,34]. But the intensity of this emission peak changes dramatically along with the polarity of the solvents. In polar solvents, such as dimethylformide (DMF), the emission intensity drops dramatically compared with that in non-polar solvents. But the fluorescence spectrum of model compound **PDI-H** does not change significantly in different solvents with different polarities. This suggests the "excited state interactions" between the PY part and PDI part within **PDI-PY** in non-polar solvents are different from that in polar solvents. This may be caused by photoinduced hole transfer from PDI to PY, which will be discussed later [21].

When the molecule of **PDI-PY** is selectively excited at 330 nm, where only the PY part absorbs light, the fluorescence of PY part of **PDI-PY** appears around 380–400 nm with very small intensity (Fig. 3B) [35–37]. Meaning while, a strong emission band appears around 560 nm, which can be assigned to the emission of PDI part of **PY-PDI**. This result suggests the presence of an efficient photoinduced energy transfer from PY to PDI within **PY-PDI** when PY is selectively excited. This is rational because of the large overlap between the emission of pyrene and the absorption of PDI as shown in Fig. 4.

Table 1
Fluorescence properties of **PDI-PY** and model compound **PY-OH** when they were excited at 330 nm.Table 1

	$\Phi_{(PDI)}$ [%][a,b]		$\Phi_{(PY)}$ [%][a,c]		Φ_q [%]		Φ_{ent} [%]		Φ_{ET} [%]	
	TOL	DMF	TOL	DMF	TOL	DMF	TOL	DMF	TOL	DMF
PY-OH	–	–	10.1	21.9	–	–	–	–		
PDI-PY	42.0	3.3	0.12	1.44	~100	90.9	98.4	24.0	–	66.9

[a] Absolute fluorescence quantum yields.
[b] Fluorescence quantum yield of the PDI emission band around 600 nm.
[c] Fluorescence quantum yield of the PY emission band around 400 nm.

3.2. The energy and electron transfer between PY and PDI within *PDI-PY* in solutions

To estimate the energy transfer efficiency (Φ_{ent}), the absolute fluorescence quantum yields and fluorescence lifetimes of **PDI-PY** and the model compounds, **PY-OH** and **PDI-H**, were measured. The results are summarized in Table 1 and 2. The absolute fluorescence quantum yields were measured by an integrating sphere on FLS 920. The fluorescence quenching efficiencies (Φ_q) were calculated by comparing the fluorescence quantum yield of PY part ($\Phi_{(PY)}$) of **PDI-PY** with that of **PY-OH** following Eq. (1).

$$\Phi_q = 1 - \frac{\Phi_{(PDI-PY,PDI,330)}}{\Phi_{(PY-OH)}} \quad (1)$$

Where $\Phi_{(PDI\text{-}PY,\ PDI,\ 330)}$ refers to the fluorescence quantum yield of PDI part within **PDI-PY** when it is excited at 330 nm, while $\Phi_{(PY\text{-}OH)}$ refers to the fluorescence quantum yield of **PY-OH**. It gives information about how much fluorescence of PY has been quenched by PDI within **PDI-PY** when PY is selectively excited. The results shown in Table 1 suggest that the fluorescence quenching of PY by PDI within **PDY-PY** in all solvents are extremely efficient and close to 100%.

The energy transfer efficiencies (Φ_{ent}) can be calculated by comparing the excitation fluorescence spectrum of **PY-PDI** with its normalized absorption spectrum as described in our or others previous papers [38,39]. But the absolute fluorescence quantum yields can be measured more easily and accurately now by the instrument, therefore, Φ_{ent} in this work were calculated by comparing the fluorescence quantum yield of PDI part of **PDI-PY** when PY subunit was selectively excited (330 nm) with that of PDI part of **PDI-PY** when PDI subunit was selectively excited (500 nm) following Eq. (2) [40].

$$\Phi_{ent} = \frac{\Phi_{(PDI-PY,\ PDI,\ 330)}}{\Phi_{(PDI-PY,\ PDI,\ 500)}} \quad (2)$$

where $\Phi_{(PDI\text{-}PY,\ PDI,\ 330)}$ refers to the fluorescence quantum yield of PDI part of **PDI-PY** when it is excited at 330 nm, while $\Phi_{(PDI\text{-}PY,\ PDI,\ 500)}$ is the fluorescence quantum yield of PDI part of **PDI-PY** when it is excited at 500 nm. The Φ_{ent} in non-polar solvent is 98%, which is almost the same as Φ_q and suggests that the energy transfer dominates the fluorescence quenching. However, in a polar solvent (DMF) Φ_{ent} is obviously smaller than the corresponding Φ_q, suggesting the presence of another fluorescence quenching process besides the energy transfer. Based on the previous research [23], we attribute this extra fluorescence quenching process to the photoinduced electron transfer from PY to PDI subunit when **PDI-PY** is selectively excited at 330 nm. To prove the presence of this electron transfer, the electrochemical properties of the model

Table 2
Fluorescence properties of **PDI-PY** and model compound **PDI-H** when they are excited at 500 nm.Table 2

	$\Phi_{(PDI)}$ [%][a,b]		Φ_q [%]		τ [ns][c]		Φ'_{ET} [%]		k'_{ET} ($\times 10^9$ S^{-1})	
	TOL	DMF	TOL	DMF	TOL	DMF	TOL	DMF	TOL	DMF
PDI-PY	42.7	13.5	56.6	85.7	1.99(τ_1) 5.24(τ_2)	0.32(τ_1) 5.12(τ_2)	56.7	85.7	0.50	3.12
PDI-H	98.5	94.7	–	–	4.73		–	–	–	–

[a] Absolute fluorescence quantum yields.
[b] Fluorescence quantum yield of the emission band of PDI around 600 nm.
[c] Fluorescence lifetimes measured for the fluorescence of PDI around 600 nm.

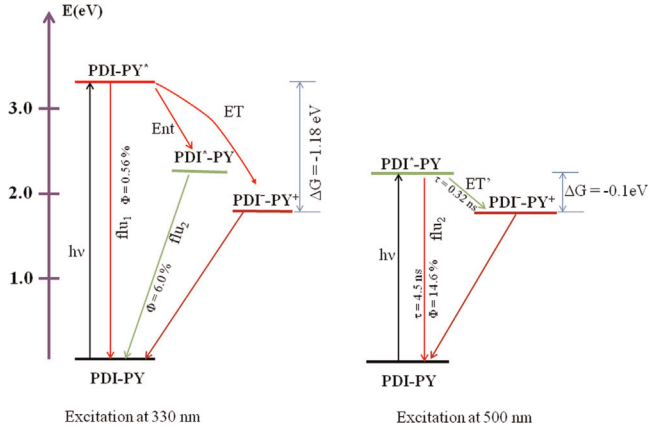

Scheme 2. Energy level diagram of **PDI-PY** and electron transfer pathways, upon excitation of the PY at 330 nm (left) and of the PDI at 500 nm (right) [22].

compounds were measured and the free energy change (ΔG_{ET}) of the electron transfer from PY to PDI within **PY-PDI** when PY was selectively excited was calculated following equation 3[41].

$$\Delta G_{ET} = E_{ox} - E_{red} - E_{0,0} \quad (3)$$

where E_{ox} and E_{red} are, respectively, the oxidation and reduction potentials of the donor PY and acceptor PDI. $E_{0,0}$ is the zero–zero transition energy of the chromophore which is selectively excited (3.29 eV for **PY-OH** and 2.21 eV for **PDI-H**). The oxidation potential of PY in dichloromethane is +0.90 V *vs* Fc/Fc^+ [22]. The reduction potential of **PDI-H** in dichloromethane is measured to be −1.21 V *vs* Fc/Fc^+ (Fig S6 in supporting information). The free energy changes of the electron transfer from PY to PDI within **PY-PDI** is then calculated to be −1.18 eV when PY is selectively excited and −0.1 eV when PDI is selectively excited. Both of them are negative and clearly indicate that the photoinduced electron transfer from PY to PDI within **PY-PDI** is thermal dynamically favorable. Moreover, similar photoinduced electron transfer processes were well documented in the previous literatures. Therefore, it is reasonable to ascribe the fluorescence quenching of PY by PDI within **PY-PDI** to photoinduced electron transfer [19–25].

The electron transfer efficiency (Φ_{ET}) can be estimated by the difference between the fluorescence quenching efficiency (Φ_q) and energy transfer efficiency (Φ_{ent})[38]. In non-polar solvents, the electron transfer from PY to PDI is negligible, but in polar solvents, the electron transfer dominates the fluorescence quenching. Principally, with the fluorescence lifetime of **PY** part of **PDI-PY**, the rate constants of both energy and electron transfer can be estimated. Unfortunately, the lifetime of PY part within **PDI-PY** can not be measured accurately by TCSPC method because of the extremely weak fluorescence intensity. This result suggests that the energy and electron transfer between PY and PDI within **PDI-PY** is extremely fast.

When **PDI-PY** was selectively excited at 500 nm, where only PDI part absorbs light, it gave the same fluorescence spectrum (Fig. 3B) as it was excited at 330 nm. The emission can be assigned similarly to the fluorescence of PDI [42]. The absolute fluorescence quantum yields and fluorescence lifetimes are summarized in Table 2. By comparing the fluorescence quantum yield of **PDI-PY** with that of the model compound **PDI-H** when they are selectively excited at 500 nm, we find that the fluorescence of PDI within **PDI-PY** is quenched significantly by PY. This fluorescence quenching can be attributed to the hole transfer (HT) from PDI to PY, in another word, the electron transfer from PY to the excited PDI (ET′) [43,44]. The efficiency of this electron transfer from PY to excited PDI (Φ'_{ET}) within **PDI-PY** can be estimated from the fluorescence quenching efficiency (Φ_q) of PDI by PY within **PDI-PY** following Eq. (4).

$$\Phi'_q = \Phi'_{ET} = 1 - \frac{\Phi'_{(PDI-PY,\ PDI,\ 500)}}{\Phi_{(PDI-H)}} \quad (4)$$

where $\Phi'_{(PDI\text{-}PY,\ PDI,\ 500)}$ is the fluorescence quantum yield of PDI part of **PDI-PY** when it is excited at 500 nm.

Meanwhile, this electron transfer rate constant (k'_{ET}) when PDI was selectively excited can be calculated from the fluorescence lifetime ($\tau_{(PDI\text{-}PY)}$) of PDI within **PDI-PY** following Eq. (5).

$$k'_{ET} = \frac{1}{\tau_{(PDI-PY)}} - \frac{1}{\tau_{(PDI-H)}} \quad (5)$$

The calculated results for both Φ'_{ET} and k'_{ET} are shown in Table 2 [40]. In polar solvent DMF, the k'_{ET} is much faster than that in a non-polar solvent because of the stabilization effects of the polar solvent to the charge separated states.

Based on the results as mentioned above, the photoinduced processes between PY and PDI within **PY-PDI** are summarized in Scheme 2. When PY is selectively excited, both energy transfer (Ent) and electron transfer (ET) from PY to PDI can happen with high efficiency. The electron transfer can be hindered by non-polar solvents. But when PDI is selectively excited, the electron transfer from PY to excited PDI (ET′) is the dominating fluorescence quenching process.

3.3. *Properties of **PDI-PY** in polymer matrixes*

Based on the results as mentioned above, we can conclude that **PDI-PY** in solution undergoes efficient energy and electron transfer after photo excitation at 330 nm. In polar solvents, the electron transfer is dominating, but in non-polar solvents, the energy transfer is preferred. Now a question is how the photophysical processes are affected by the environment of polymer matrixes? To answer this question, the spectroscopic properties of **PDI-PY** were also measured in PS and PMMA films.

The absorption spectrum of **PDI-PY** in polystyrene (PS) is shown in Fig. 5. The absorption spectrum of **PDI-PY** is identical to the sum of the absorption spectra of the model compounds **PY-OH**

and **PDI-H**. This means there is no ground state interactions between PY and PDI subunits within **PDI-PY** in PS matrix.

The fluorescence spectrum of **PDI-PY** in PS film with excitation at 330 nm is shown in Fig. 6. The spectrum is dominated by the emission of PDI, suggesting the presence of energy transfer from PY to PDI within **PDI-PY**, in consistent with that observed in solutions.

3.4. The energy and electron transfer within PDI-PY in polymer matrixes

To calculate the energy transfer efficiency, the fluorescence quantum yields and lifetimes were measured for the PY and PDI subunits of **PDI-PY**. The results are summarized in Tables 3 and 4.

The fluorescence quenching efficiency of PY by PDI within **PDI-PY** in the PS film is 78.0%, which is efficient, but still smaller than that in solutions (~100%). This means that the fluorescence quenching process in PS film is slower than that in solutions. The energy transfer efficiency (Φ_{ent}) is calculated by comparing the fluorescence quantum yield of PDI part within **PY-PDI** when it is selectively excited at 330 nm with the fluorescence quantum yield of PDI part when **PY-PDI** is selectively excited at 500 nm following Eq. (1). In the PS film, Φ_{ent} is calculated to be 76.1%, which is also smaller than that measured for **PDI-PY** in toluene. This result suggests that the energy transfer in the PS film is slower and less efficient than that in toluene. The efficiency of Förster type energy transfer is affected by the mutual orientation of donor and acceptor [44]. The optimized conformation for efficient energy transfer can be easily achieved by the rotation of the covalent bonds in solution. But the conformation of **PDI-PY** is frozen by the rigid environment of the PS film. The PDI and PY subunits can not adapt an optimized conformation for the Förster type energy transfer, and hence the energy transfer is less efficient than that in solutions. In the PS film, the energy transfer is a dominating process of the fluorescence quenching because the energy transfer efficiency (76.1%) is similar to the fluorescence quenching efficiency (78.0%). This result is similar with that found for **PDI-PY** in toluene.

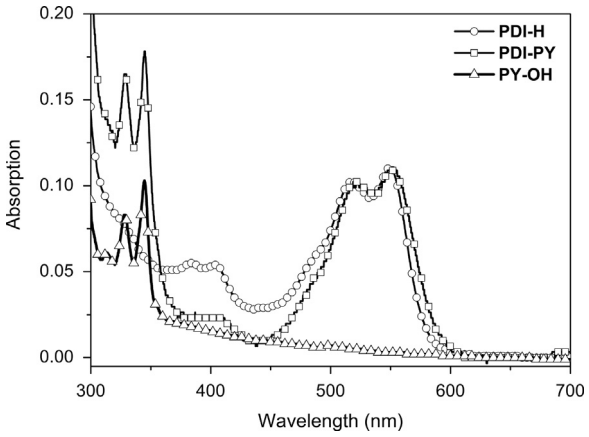

Fig. 5. Normalized absorption spectra of **PDI-PY**, **PDI-H,** and **PY-OH** in PS films.

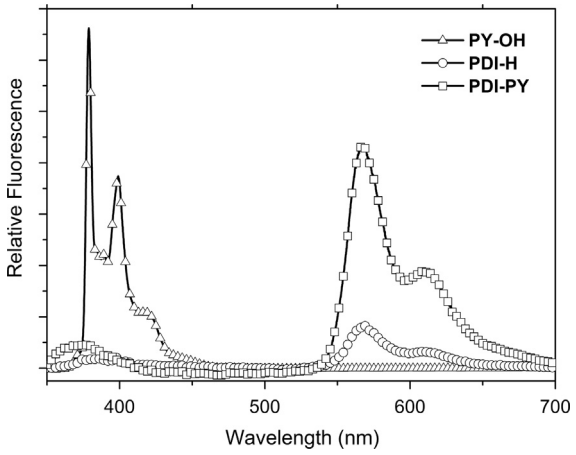

Fig. 6. Fluorescence spectra of **PDI-PY**, **PDI-H**, and **PY-OH** in PS films excited at 330 nm.

When **PDI-PY** is selectively excited at 500 nm, the fluorescence of PDI unit of **PDI-PY** is also similarly quenched by the PY subunit as that observed for **PDI-PY** in solutions. This fluorescence quenching suggests the presence of electron transfer from PY to excited PDI within **PDI-PY** in the PS film. However, this electron transfer efficiency calculated from the fluorescence quenching efficiency is 6.4% in the PS film, which is much smaller than that in the toluene solution (56.7%). This result is surprising at the first glance, because the polarity of the PS film is similar with that of toluene. But the rigid environment of the PS film exhibits extremely large re-organization energy, therefore, it can not provide efficient stabilization for the product of the electron transfer and then the electron transfer between PY and PDI subunit within **PDI-PY** is remarkably hindered [45].

In the PMMA thin film, the absorption spectra of model compounds **PY-OH** and **PDI-H** as well as **PDI-PY** revealed no ground state interactions between PY and PDI subunits as shown in Fig. S4 in Supplementary material. The fluorescence spectra of them as shown in Fig. S4 indicate the presence of energy transfer from PY to PDI unit. But the energy transfer efficiency (Φ_{ent}) is calculated to be 38.3%, which is much smaller than that in the PS film. The efficiency of electron transfer from PY to PDI subunit within **PDI-PY** when PY is selectively excited, however, is much bigger than that in the PS film, this can be ascribed to the polar environment in PMMA. It is worth noting that the electron transfer efficiency in the PMMA film is much smaller than that in polar solvent DMF. This might be caused also by the rigid environment in PMMA, which causes larger re-organization energy for the solvation of the charge separated states and then reduces the free energy change of the electron transfer following the Marcus theory [45]. The efficiency of the electron transfer when PDI is selectively excited, which is calculated from the lifetimes, reveals also that the polar

Table 3
Fluorescence properties of **PDI-PY** and model compound **PY-OH** when they were excited at 330 nm.Table 3

	$\Phi_{(PDI)}$ [%][a,b]		$\Phi_{(PY)}$ [%][a,c]		Φ_q [%]		Φ_{ent} [%]		Φ_{ET} [%]	
	PS	PMMA	PS	PMMA	PS	PMMA	PS	PMMA	PS	PMMA
PY-OH	–	–	42.9	28.9	–	–	–	–		
PDI-PY	69.7	21.7	9.4	14.0	78.0	51.5	76.1	38.3	–	13.2

[a] Absolute fluorescence quantum yields.
[b] Fluorescence quantum yield of the PDI emission band around 600 nm.
[c] Fluorescence quantum yield of the PY emission band around 400 nm.

Table 4
Fluorescence properties of **PDI-PY** and model compound **PDI-H** when they were excited at 500 nm.Table 4

	$\Phi'_{(PDI)}$ [%][a,b]		Φ'_q [%]		τ[ns][c]		Φ'_{ET} [%]		k'_{ET}($\times 10^9$ S^{-1})	
	PS	PMMA	PS	PMMA	PS	PMMA	PS	PMMA	PS	PMMA
PDI-PY	91.6	53.04	6.4	33.1	4.51(τ_1) 14.01(τ_2)	0.17(τ_1) 5.59(τ_2)	6.4	33.1	0	5.7
PDI-H	97.8	79.3	–	–	5.24	5.15	–	–	–	–

[a] Absolute fluorescence quantum yields.
[b] Fluorescence quantum yield of the emission band of PDI around 600 nm.
[c] Fluorescence lifetimes measured for the fluorescence of PDI around 600 nm.

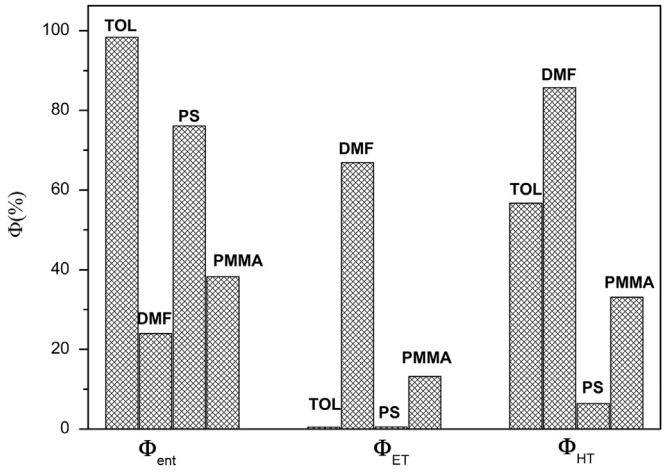

Fig. 7. Comparison of the efficiencies of the energy transfer (Φ_{ent}), electron transfer when PY is excited (Φ_{ET}), and electron transfer when PDI is excited (Φ'_{ET}) between PY and PDI within **PDI-PY** in different environments.

environment of PMMA provides a better place for the electron transfer than PS does. But the electron transfer efficiency is still smaller than that in nonpolar solvents, such as toluene.

The comparison of the electron and energy transfer efficiencies in solutions with that in polymer matrixes is shown in Fig. 7. In a non-polar film, such as the PS film, the energy transfer efficiency decreases a little, while the electron and hole transfer processes are almost completely hindered. But in a polar film, such as the PMMA film, the efficiency of energy transfer increases significantly while the efficiencies of hole transfer and electron transfer decrease significantly with respect to those in polar solvents. Comparing with that in the PS film, the energy transfer efficiency is smaller, but the electron transfer efficiencies are much larger in the PMMA film. This difference between the PS film and the PMMA film indicates that the PMMA film can still provide stabilization to the charge separated states produced by electron transfer even though the rigid environment in it.

4. Conclusion

The intramolecular photoinduced electron and energy transfer between PY and PDI within **PDI-PY** are comparatively studied by steady state absorption and fluorescence spectra, as well as time resolved fluorescence spectra. The results revealed the presence of competition between the photoinduced energy and electron transfer from PY subunit to PDI subunit within **PDI-PY** when PY is selectively excited. In non-polar solvents, the photoinduced energy transfer dominates the fluorescence quenching while in polar solvents, the electron transfer is the dominant. When the molecule of **PDI-PY** is embedded in a non-polar polymer matrix, such as PS, the energy transfer dominates the fluorescence quenching, while the electron transfer is almost completely hindered. In the polar PMMA film, the energy transfer is still a dominating fluorescence quenching process, even though the efficiency dropped remarkably. The electron transfer are hindered compared with that in solutions, but enhanced in comparison with that in the PS film. The results of this research suggests that rigid environment of polymer matrixes favors energy transfer, rather than a competition electron transfer. Polymer matrixes are probably ideal medium for constructing light-harvesting systems if electron transfer is needed to be avoid.

Acknowledgments

We thank the Natural Natural Science Foundation of China (with Grand nos. 91233108, 21173136) for the financial support.

Appendix A. Supplementary information

Supplementary data associated with this article can be found in the online version at doi:10.1016/j.jlumin.2015.07.046

References

[1] M.R. Wasielewski, J. Org. Chem. 71 (2006) 5051.
[2] P.K. Dutta, J. Phys. Chem. Lett. 2 (2011) 467.
[3] L. Sang, Y. Zhao, C. Burda, Chem. Rev. 114 (2014) 9283.
[4] P.V. Kamat, J. Phys. Chem. C 111 (2007) 2834.
[5] A. Listorti, B. O´Regan, J.R. Durrant, Chem. Mater. 23 (2011) 3381.
[6] S.G. Kumar, L.G. Devi, J. Phys. Chem. A 115 (2011) 13211.
[7] (a) M. Supur, S. Fukuzumi, J. Am. Chem. Soc. 124 (2002) 9582;
(b) M. Supur, Y.M. Sung, D. Kim, S. Fukuzumi, J. Phys. Chem. C 117 (2013) 12438.
[8] M.T. Vagnini, A.L. Smeigh, J.D. Blakemore, S.W. Eaton, N.D. Schley, F.D. Souza, R.H. Crabtree, G.W. Brudvig, D.T. Co, M.R. Wasielewski, Proc. Natl. Acad. Sci. USA 109 (2012) 15651.
[9] G. Bottari, G.D. Torre, D.M. Guldi, T. Torres, Chem. Rev. 110 (2010) 6768.
[10] S. Verma, H.N. Ghosh, J. Phys. Chem. Lett. 3 (2012) 18771.
[11] (a) M.R. Wasielewski, Chem. Rev. 92 (1992) 435;
(b) D. Gust, T.A. Moore, A.L. Moore, Acc. Chem. Res. 26 (1993) 198;
(c) D. Gust, T.A. Moore, A.L. Moore, Acc. Chem. Res. 34 (2001) 40.
[12] (a) O.A. Bozdemir, R. Guliyev, O. Buyukcakir, S. Selcuk, S. Kolemen, G. Gulseren, T. Nalbantoglu, H. Boyaci, E.U. Akkaya, J. Am. Chem. Soc. 132 (2010) 8029;
(b) A. Coskun, E. Deniz, E.U. Akkaya, Org. Lett. 7 (2005) 5187;
(c) A.P. de Silva, N.D. McClenaghan, Chem. Eur. J 8 (2002) 4935.
[13] (a) H.X. Wang, X.Y. Li, Org. Biomol. Chem. 9 (2011) 5436;
(b) H.X. Wang, H.X. Wu, L. Xue, D.L. Wang, X.Y. Li, Org. Biomol. Chem. 8 (2010) 1017.
[14] D.Z. Shen, L.S. Wang, Z.X. Pan, S. Cheng, X.L. Zhu, L.J. Fan, Macromolecules 44 (2011) 1009.
[15] A. Jacobson, A. Petric, D. Hogenkamp, A. Sinur, J.R. Barrio, J. Am. Chem. Soc. 118 (1996) 5572.
[16] U. Narang, C.F. Zhao, J.D. Bhawalkar, F.V. Bright, P.N. Prasad, J. Phys. Chem. 100 (1996) 4521.
[17] S.A. Ruetten, J.K. Thomas, J. Phy. Chem. B 102 (1998) 598.
[18] P. Hrdlovič, J. Kollár, Š. Chmela, J. Photochem. Photobio. A: Chem. 163 (2002) 289.
[19] (a) A. Sautter, B.K. Kaletas, D.G. Schmid, R. Dobrawa, M. Zimine, G. Jung, I.H. M. van Stokkum, L.D. Cola, R.M. Williams, F. Würthner, J. Am. Chem. Soc.

127 (1965) 6719;
(b) F. Würthner, A. Sautter, Org. Biomol. Chem. 1 (2003) 240.
[20] W.J. Shumate, D.L. Mattern, A. Jaiswal, D.A. Dixon, T.R. White, J. Burgess, A. Honciuc, R.M. Metzger, J. Phys. Chem. B 110 (2006) 11146.
[21] J.H. Wan, Z. Ma, F. Liu, Z. Xu, H.Y. Wang, H.J. Jiang, W. Huang, J. Photochem. Photobiol. A 211 (2010) 115.
[22] N.V. Anh, F. Schlosser, M.M. Groeneveld, I.H.M. van Stokkum, F. Würthner, R.M. Williams, J. Phys. Chem. C 113 (2009) 18358.
[23] B.K. Kaletas, R. Dobrawa, A. Sautter, F. Würthner, M. Zimine, L.D. Cola, R. M. Williams, J. Phys. Chem. A 108 (2004) 1900.
[24] C.C. You, C. Hippius, M. Grüne, F. Würthner, Chem. Eur. J 12 (2006) 7510.
[25] Y.J. Li, H. Li, Y.L. Li, H.B. Liu, S. Wang, X.R. He, N. Wang, D.B. Zhu, Org. Lett. 7 (2005) 4835.
[26] C.T. Zhao, Y.X. Zhang, R.J. Li, X.Y. Li, J.Z. Jiang, J. Org. Chem. 72 (2007) 2402.
[27] Y. Shi, H.X. Wu, L. Xue, X.Y. Li, J. Colloid Interface Sci. 365 (2012) 172.
[28] (a) H.Y. Liu, L. Shen, Z.Z. Cao, X.Y. Li, Phys. Chem. Chem. Phys. 16 (2014) 16399;
(b) G.J. Qi, L.L. Jiang, Y.Y. Zhao, Y.Q. Yang, X.Y. Li, Phys. Chem. Chem. Phys. 15 (2013) 17342.
[29] (a) K. Balakrishnan, A. Datar, T. Naddo, J. Huang, R. Oitker, M. Yen, J. Zhao, L. Zang, J. Am. Chem. Soc. 128 (2006) 7390;
(b) Y. Che, A. Datar, X. Yang, T. Naddo, J. Zhao, L. Zang, J. Am. Chem. Soc. 129 (2007) 6354.
[30] (a) W. Wang, L.-S. Li, G. Helms, H.-H. Zhou, A.D.Q. Li, J. Am. Chem. Soc. 125 (2003) 1120;
(b) W. Wang, L.Q. Wang, B.J. Palmer, G.J. Exarhos, A.D.Q. Li, J. Am. Chem. Soc. 128 (2006) 11150.
[31] C.X. Yao, H.-B. Kraatz, R.P. Steer, Photochem. Photobiol. Sci. 4 (2005) 191.
[32] A.G. Crawford, A.D. Dwyer, Z.Q. Liu, A. Steffen, A. Beeby, L.-O. Palsson, D. J. Tozer, T.B. Marder, J. Am. Chem. Soc. 133 (2011) 13349.
[33] J. Feng, B. Liang, D. Wang, H. Wu, L. Xue, X. Li, Langmuir 24 (2008) 11209.
[34] F. Würthner, Chem. Commun. (2004) 1564.
[35] R. Katoh, K. Suzuki, A. Furube, M. Kotani, K. Tokumaru, J. Phys. Chem. C 113 (2009) 2961.
[36] Y. Niko, S. Kawauchi, S. Otsu, K. Tokumaru, G.-I. Konishi, J. Org. Chem. 78 (2013) 3196.
[37] G. Venkataramana, S. Sankararaman, Eur. J. Org. Chem. 19 (2005) 4162.
[38] A.C. Ng, X.Y. Li, D.K.P. Ng, Macromolecules 32 (1999) 5292.
[39] P.S. Reeta, R.K. Kanaparthi, L. Giribabu, J. Chem. Sci. 125 (2013) 259.
[40] W. Xu, H.L. Chen, Y.F. Wang, C.T. Zhao, X.Y. Li, S.Q. Wang, Y.X. Weng, ChemPhyChem 9 (2008) 1409.
[41] L. Giribabu, P.S. Reeta, R.K. Kanaparthi, M. Srikanth, J. Phys. Chem. A 117 (2013) 2944.
[42] J.Q. Feng, Y.X. Zhang, C.T. Zhao, R.J. Li, W. Xu, X.Y. Li, J.Z. Jiang, Chem. Eur. J 14 (2008) 7000.
[43] (a) X.Y. Li, Q.F. Zhou, H.J. Xu, Chin. J. Chem. 16 (1998) 97;
(b) X. Li, D.K.P. Ng, Eur. J. Inorg. Chem. 8 (2000) 1845.
[44] N.J. Turro, Modern Molecular Photochemistry, Benjamin/Cummings, Menlo Park, 1978.
[45] R.A. Marcus, J. Chem. Phys. 43 (1965) 679.